Continuum Mech. Thermodyn. (2005) 17: 43–50
Digital Object Identifier (DOI) 10.1007/s00161-004-0186-0

Original article

Failures of the Burnett and super-Burnett equations in steady state processes

H. Struchtrup

Department of Mechanical Engineering, University of Victoria, PO Box STN CSC 3055, Victoria BC V8W 3P6, Canada
(e-mail: struchtr@uvic.ca)

Received March 30, 2004 / Accepted April 22, 2004
Published online February 22, 2005 –
Communicated by G. M. Kremer

Abstract. Linearized Burnett and super-Burnett equations are considered for steady state Couette flow. It is shown that the linear super-Burnett equations lead to periodic velocity and temperature curves, i.e. unphysical solutions. The problem is discussed as well for the so-called augmented Burnett equations by Zhong et al. (AIAA Journal **31**, 1036-1043 (1993)), and for the recently introduced regularized 13 moment equations (R13) of Struchtrup and Torrilhon (Phys. Fluids **15**(9), 2668–2680 (2003)). It is shown that both theories exhibit proper Knudsen boundary layers for velocity and temperature. However, the heat flux parallel to the wall has different signs for the Burnett and the R13 equations, and a comparison with DSMC results shows that only the R13 equations predict the proper sign.

Key words: rarefied gas flows, kinetic theory, boundary layers, super-Burnett equations, regularized 13 moment equations
PACS: 51.10.-y, 47.45.-n

1 Introduction

The laws of Navier-Stokes and Fourier (NSF) are applicable only for flows at sufficiently small Knudsen numbers, and fail in the description of flows at Knudsen numbers $\mathrm{Kn} \gtrsim 0.05$ (say). These Knudsen numbers are easily reached nowadays, e.g. in microscopic flows, or in high altitude flight, and a reliable set of equations that can be solved at low computational cost for the description of these flows is highly desirable. Note that Bird's direct simulation Monte Carlo method [1] allows accurate computations, but still requires extreme computational time, while a set of differential equations in general can be solved faster.

The NSF equation result from the Chapman-Enskog expansion of the Boltzmann equation where the Knudsen number is the relevant smallness parameter. Thus, one might expect the next orders of the expansion, the Burnett and super-Burnett equations [2,3], to be better suited for the description of flows at larger Knudsen numbers. However, as was shown by Bobylev [4], the Burnett and super-Burnett equations are unstable, so that small wavelength fluctuations will blow up in time. Also, as was shown recently [5], small oscillations in time at a given space point will lead to large oscillations at other points.

Obviously, these stability problems are not relevant when one considers steady state solutions of the Burnett and super-Burnett equations as was done in [6–8] for micro flows, and in [9] for shock waves. The applications to steady state rely on the assumption that the Burnett and super-Burnett equations do not capture the time behavior well, hence the instabilities, but are accurate for the description of space variations in steady state.

This assumption becomes doubtful due to problems in computing meaningful shock structures from the Burnett equations, where the non-linear terms seem to cause instabilities in the numerical solution of the equations [9]. Zhong et al. introduced terms of super-Burnett order into the Burnett equations, and their "augmented Burnett" equations [10,11] yield stability in time (no blow up of small wavelength oscillations), and facilitate the computation of shock structures, but they are unstable in space (blow up of high frequency oscillations) [12].

Recently Struchtrup and Torrilhon derived a new set of equations of super-Burnett order [5,12] from a regularization of Grad's 13 moment equations [13]. The new equations termed as "regularized 13 moment equations", or "R13 equations", are derived from a Chapman-Enskog like expansion of an extended set of moment equations which in turn are based on the Boltzmann equation.

Just recently, in [14], an alternative derivation was presented, which is solely based on considerations of the order of magnitude of the moments of the phase density, and the order of accuracy of the transport equations, both measured in powers of the Knudsen number. This method is independent from the Grad method, and quite different from the Chapman-Enskog method, with which it shares some similarity, however. In [14] the new method is developed up to the third order in the Knudsen number, and it is shown that it yields the Euler equations at zeroth order, the Navier-Stokes-Fourier equations at first order, Grad's 13 moment equations (with omission of a non-linear term) at second order, and the R13 equations at third order.

It could be shown that the R13 equations are linearly stable, that their predictions for phase speed and damping of ultrasound waves agree well with measurements [5], and that the equations yield smooth meaningful shock structures[12].

Moreover, it was shown that the R13 equations allow the description of linear Knudsen boundary layers in principle, although it is unclear at present how boundary conditions can be prescribed for the moments. The super-Burnett equations as well as the augmented Burnett equations face the same difficulties in prescribing boundary conditions. Nevertheless, these equations can be tested for their ability to describe linear Knudsen layers, and that is the topic of this note.

We shall consider linearized Burnett, super-Burnett and augmented Burnett equations for the case of steady state Couette flow, and shall show that the super-Burnett equations do not predict Knudsen boundary layers but unphysical oscillations in space. This renders them unsuitable as a tool for the description of micro flows. The augmented Burnett equations yield Knudsen boundary layers, but are criticized for not being derived in a rational manner. We repeat the analysis of the R13 equations for the same problem, and discuss the Knudsen boundary layers.

Special attention is given to the heat flux parallel to the wall, which the linearized R13 equations and the Burnett equations predict with different signs. The comparison with Direct Simulation Monte Carlo results shows that the linearized R13 equations meets the numerical experiment, so that the linearized Burnett equations (and the augmented Burnett equations) fail in the proper description of this phenomenon.

2 Burnett, super-Burnett, and augmented Burnett equations

We shall use dimensionless coordinates and variables throughout the paper, and consider only small deviations from an equilibrium ground state with mass density ρ_0, temperature T_0 and zero velocity, $v_{i,0} = 0$. σ_{ij} and q_i denote the trace free part of the stress tensor and the heat flux, respectively. Dimensionless variables $\hat{\varrho},\ \hat{T},\ \hat{v}_i,\ \hat{\sigma}_{ij},\ \hat{q}_i$ are introduced as

$$\varrho = \varrho_0 \left(1 + \hat{\varrho}\right) \ , \ \ T = T_0 \left(1 + \hat{T}\right) \ , \ \ v_i = \sqrt{RT_0}\hat{v}_i \ , \ \ \sigma_{ij} = \varrho_0 RT_0 \hat{\sigma}_{ij} \ , \ \ q_i = \varrho_0 \sqrt{RT_0}^3 \hat{q}_i \ ,$$

R is the gas constant. Moreover, we identify a relevant length scale L of the process, and use it to non-dimensionalize the space and time variables according to

$$x_i = L\hat{x}_i \ , \ \ t = \frac{L}{\sqrt{RT_0}}\hat{t} \ .$$

The corresponding dimensionless collision time is then given by the Knudsen number

$$\mathrm{Kn} = \frac{\mu_0}{\rho_0 \sqrt{RT_0} L} \ , \tag{2.1}$$

where μ_0 denotes the viscosity of the ground state.

For notational convenience, we shall drop the hats on the variables in the sequel. After linearizing in the variables the conservation laws for mass momentum and energy read

$$\frac{\partial \rho}{\partial t}+\frac{\partial v_k}{\partial x_k}=0\ ,$$
$$\frac{\partial v_i}{\partial t}+\frac{\partial \rho}{\partial x_i}+\frac{\partial T}{\partial x_i}+\frac{\partial \sigma_{ik}}{\partial x_k}=0\ ,$$
$$\frac{3}{2}\frac{\partial T}{\partial t}+\frac{\partial q_k}{\partial x_k}+\frac{\partial v_k}{\partial x_k}=0\ ,$$

and these must be closed by a suitable set of equations for stress σ_{ij} and heat flux q_i. The Chapman-Enskog expansion yields

$$\sigma_{ij}=\sigma_{ij}^{(0)}+\mathrm{Kn}\sigma_{ij}^{(1)}+\mathrm{Kn}^2\sigma_{ij}^{(2)}+\mathrm{Kn}^3\sigma_{ij}^{(3)}+\cdots\ ,$$
$$q_i=q_i^{(0)}+\mathrm{Kn}q_i^{(1)}+\mathrm{Kn}^2q_i^{(2)}+\mathrm{Kn}^3q_i^{(3)}+\cdots\ ,$$

where, after linearization,

$$\sigma_{ij}^{(0)}=q_i^{(0)}=0\ . \tag{2.2}$$

$$\sigma_{ij}^{(1)}=-2\frac{\partial v_{\langle i}}{\partial x_{j\rangle}}\quad\text{and}\quad q_i^{(1)}=-\frac{15}{4}\frac{\partial T}{\partial x_i}\ , \tag{2.3}$$

$$\sigma_{ij}^{(2)}=-2\frac{\partial^2 \rho}{\partial x_{\langle i}\partial x_{j\rangle}}+\frac{\partial^2 T}{\partial x_{\langle i}\partial x_{j\rangle}}\quad\text{and}\quad q_i^{(2)}=-\frac{13}{4}\frac{\partial^2 v_k}{\partial x_k\partial x_i}+\frac{3}{2}\frac{\partial^2 v_i}{\partial x_k\partial x_k}\ , \tag{2.4}$$

$$\sigma_{ij}^{(3)}=\frac{5}{3}\frac{\partial^2}{\partial x_{\langle i}\partial x_{j\rangle}}\frac{\partial v_k}{\partial x_k}-\frac{4}{3}\frac{\partial^2}{\partial x_k\partial x_k}\frac{\partial v_{\langle i}}{\partial x_{j\rangle}}\quad\text{and}\quad q_i^{(3)}=-\frac{157}{16}\frac{\partial^3 T}{\partial x_i\partial x_k\partial x_k}-\frac{5}{8}\frac{\partial^3 \rho}{\partial x_i\partial x_k\partial x_k}\ . \tag{2.5}$$

Here, indices in angular brackets denote the tracefree symmetric part of an tensor. Considering only the zeroth order terms (2.2) yields the Euler equations, the first order terms (2.3) are the Navier-Stokes-Fourier equations [2], addition of the second order terms (2.4) yields the Burnett equations [2], and inclusion of the third order terms (2.5) yields the super-Burnett equations [2,3,5].

The augmented Burnett equations of Zhong et al. replace the super-Burnett terms (2.5) by

$$\sigma_{ij}^{(a)}=\frac{1}{3}\frac{\partial^2}{\partial x_k\partial x_k}\frac{\partial v_{\langle i}}{\partial x_{j\rangle}}\quad\text{and}\quad q_i^{(a)}=\frac{11}{16}\frac{\partial^3 T}{\partial x_i\partial x_k\partial x_k}-\frac{5}{8}\frac{\partial^3 \rho}{\partial x_i\partial x_k\partial x_k}\ . \tag{2.6}$$

Here, the expression for $\sigma_{ij}^{(a)}$ is an ad-hoc extension to three dimensions of the proper expression in one dimension, $\sigma_{11}=\frac{2}{9}\frac{\partial^3 v}{\partial x^3}$. However, $(2.6)_1$ does not agree with the proper three dimensional term in (2.5). In the heat flux contribution $q_i^{(a)}$, the factor $\left(-\frac{157}{16}\right)$ is replaced by a factor with a different sign $\left(\frac{11}{16}\right)$. This factor goes back to the super-Burnett calculations of Wang-Chang [15], but finds no support in newer calculations of the super-Burnett coefficients [3,4,9,5].

3 Couette flow with Burnett models

We consider the steady state Couette flow problem: two infinite, parallel plates move in the $\{x_2,x_3\}$-plane with different speeds in x_2 direction. The plate distance is $L=1$ in dimensionless units, and the plates have different temperatures. In this setting, we expect that all variables will depend only on the coordinate $x_1=x$. Since matter cannot pass the plates, we will have $v_1=0$. Moreover, for symmetry reasons, there will be no fluxes in the x_3 direction, so that

$$v_i=\{0,v(x),0\}\ \text{and}\ q_3=\sigma_{13}=\sigma_{23}=0\ .$$

Under these assumptions, the mass balance is identically fulfilled, and the conservation laws reduce to

$$\frac{\partial \rho}{\partial x}+\frac{\partial T}{\partial x}+\frac{\partial \sigma_{11}}{\partial x}=0\ ,\ \frac{\partial \sigma_{12}}{\partial x}=0\ ,\ \frac{\partial q_1}{\partial x}=0\ . \tag{3.1}$$

The last two equations yield that σ_{12} and q_1 are constants of integration,

$$\sigma_{12}=const.\quad,\quad q_1=const\ .$$

The conservation laws must be furnished with the expressions for σ_{11}, σ_{12}, and q_1 and boundary conditions according to the different theories.

3.1 Navier-Stokes-Fourier equations

For the NSF equations (2.3), we obtain

$$\sigma_{11}=0\ \ ,\ \ \sigma_{12}=-\mathrm{Kn}\frac{\partial v}{\partial x}\ ,\ q_1=-\frac{15}{4}\mathrm{Kn}\frac{\partial T}{\partial x}\ ,\ \ q_2=0\ .$$

Insertion into the balance laws and integration yields

$$v=v_0-\sigma_{12}\frac{x}{\mathrm{Kn}}\ \ ,\ \ T=T_0-\frac{4}{15}q_1\frac{x}{\mathrm{Kn}}\ \ ,\ \ \rho=\rho_0-\frac{4}{15}q_1\frac{x}{\mathrm{Kn}}\ ,$$

where v_0, T_0, ρ_0 are constants of integration. Accordingly, all profiles are linear, and the variation in density is due solely to heat transfer.

In particular we note that $\sigma_{11}=q_2=0$ for the NSF equations. Non-zero values for the anisotropic contribution to pressure σ_{11} and the heat flux parallel to the wall q_2 appear only in higher order theories. DSMC calculations show non-zero values for these quantities at larger Knudsen numbers (above $\sim$0.05), and this agrees with the expectation that the NSF equations are limited to small Knudsen numbers.

3.2 Burnett equations

Now, the conservation laws (3.1) are furnished with the Burnett expressions

$$\sigma_{11}=-\frac{4}{3}\mathrm{Kn}^2\frac{\partial^2\rho}{\partial x^2}+\frac{2}{3}\mathrm{Kn}^2\frac{\partial^2 T}{\partial x^2}\ \ ,\ \ \sigma_{12}=-\mathrm{Kn}\frac{\partial v}{\partial x}\ ,$$
$$q_1=-\frac{15}{4}\mathrm{Kn}\frac{\partial T}{\partial x},\ \ q_2=\frac{3}{2}\mathrm{Kn}^2\frac{\partial^2 v}{\partial x^2}\ .$$

This implies right away that

$$v\left(x\right)=v_0-\sigma_{12}\frac{x}{\mathrm{Kn}}\ \ ,\ T\left(x\right)=T_0-\frac{4}{15}q_1\frac{x}{\mathrm{Kn}}\ \ ,\ \ q_2=0\ ,$$

where v_0,σ_{12},T_0,q_1 are constants of integration. That is the Burnett equations do not predict boundary layers for velocity and temperature, and no heat flux parallel to the wall. Note that this statement refers only to the linearized Burnett equations. Indeed, it is well known that the full Burnett equations predict the heat flux parallel to the wall as $q_2=\frac{\mu^2}{\rho T}\frac{105}{8}\frac{\partial v_i}{\partial x_k}\frac{\partial T}{\partial x_k}$.

The equations for ρ and σ_{11} lead to Knudsen layer solutions for density and stress σ_{11}, viz

$$\rho=\rho_0+\frac{4}{15}\frac{q_1}{\mathrm{Kn}}x+A\sinh\left[\frac{\sqrt{3}}{2}\frac{x-\frac{1}{2}}{\mathrm{Kn}}\right]+B\cosh\left[\frac{\sqrt{3}}{2}\frac{x-\frac{1}{2}}{\mathrm{Kn}}\right],$$
$$\sigma_{11}=-A\sinh\left[\frac{\sqrt{3}}{2}\frac{x-\frac{1}{2}}{\mathrm{Kn}}\right]-B\cosh\left[\frac{\sqrt{3}}{2}\frac{x-\frac{1}{2}}{\mathrm{Kn}}\right]\ \ .$$

Thus, in comparison to the NSF equations, the linear Burnett equations do only lead to smaller changes in the prediction of Couette flow. In particular we point out their failure to predict a heat flux parallel to the wall ($q_2=0$), and to predict boundary layers for temperature and velocity. Indeed, these appear only at the next order of approximation, which is studied now.

3.3 Super-Burnett and augmented Burnett equations

For linear Couette flow, the super-Burnett equations reduce to

$$\sigma_{11}=-\frac{4}{3}\mathrm{Kn}^2\frac{\partial^2\rho}{\partial x^2}+\frac{2}{3}\mathrm{Kn}^2\frac{\partial^2 T}{\partial x^2}\ \ ,\ \ \sigma_{12}=-\mathrm{Kn}\frac{\partial v}{\partial x}-\frac{2}{3}\mathrm{Kn}^3\frac{\partial^3 v}{\partial x^3}\ ,$$
$$q_1=-\frac{15}{4}\mathrm{Kn}\frac{\partial T}{\partial x}-\frac{157}{16}\mathrm{Kn}^3\frac{\partial^3 T}{\partial x^3}-\frac{5}{8}\mathrm{Kn}^3\frac{\partial^3\rho}{\partial x^3}\ ,\ \ q_2=\frac{3}{2}\mathrm{Kn}^2\frac{\partial^2 v}{\partial x^2}\ . \tag{3.4}$$

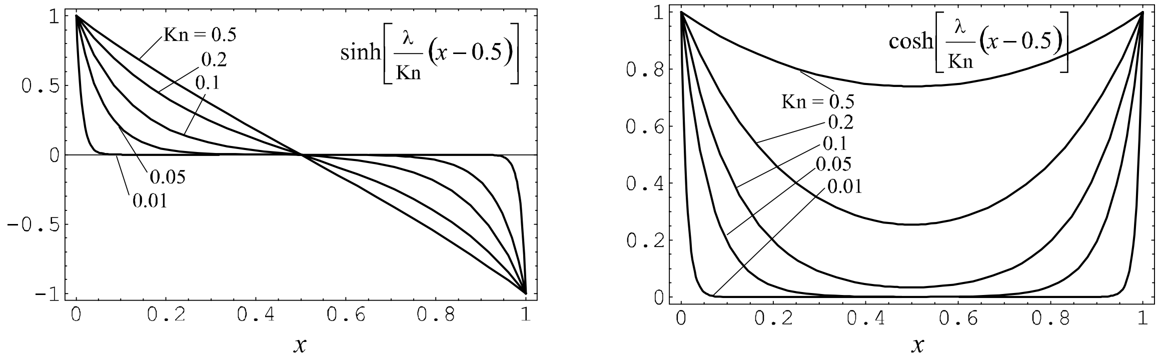

Fig. 1. Boundary layer functions $\sinh[\lambda x/\mathrm{Kn}]$ and $\cosh\,[\lambda x/\mathrm{Kn}]$ for various Knudsen numbers

For the augmented Burnett equations, the expressions for σ_{11} and q_2 remain unchanged, while the expressions for σ_{12} and q_1 read

$$\sigma_{12|aB} = -\mathrm{Kn}\frac{\partial v}{\partial x} + \frac{1}{6}\mathrm{Kn}^3\frac{\partial^3 v}{\partial x^3}\ ,\ q_{1|aB} = -\frac{15}{4}\mathrm{Kn}\frac{\partial T}{\partial x} + \frac{11}{16}\mathrm{Kn}^3\frac{\partial^3 T}{\partial x^3} - \frac{5}{8}\mathrm{Kn}^3\frac{\partial^3 \rho}{\partial x^3}\ . \tag{3.5}$$

Due to the simple structure of the linear equations, the velocity can be computed separately as

$$v_{|SB} = v_0 - \sigma_{12}\frac{x}{\mathrm{Kn}} + A\cos\left[\sqrt{\tfrac{3}{2}}\tfrac{x-\frac{1}{2}}{\mathrm{Kn}}\right] + B\sin\left[\sqrt{\tfrac{3}{2}}\tfrac{x-\frac{1}{2}}{\mathrm{Kn}}\right]\ , \tag{3.6}$$

$$v_{|aB} = v_0 - \sigma_{12}\frac{x}{\mathrm{Kn}} + A\cosh\left[\sqrt{6}\tfrac{x-\frac{1}{2}}{\mathrm{Kn}}\right] + B\sinh\left[\sqrt{6}\tfrac{x-\frac{1}{2}}{\mathrm{Kn}}\right]\ , \tag{3.7}$$

for super-Burnett and augmented Burnett equations, respectively. The constants of integration v_0, σ_{12}, A, B must be related to boundary conditions, a problem that we shall ignore here. What is important to us is the general structure of the solutions: Both sets of equations yield the linear Navier-Stokes solution $v_0 - \sigma_{12}\frac{x}{\mathrm{Kn}}$ plus a correction. However, the correction is periodic in space for the super-Burnett equations (3.6), but relates to Knudsen boundary layers for the augmented Burnett equations (3.7). Thus the change in sign at the third order derivative in σ_{12} between (3.4) and (3.5) has severe impact on the solution behavior - the super-Burnett equations yield results that are unphysical, but the solution of the augmented Burnett equations might have support in physics.

Figure 1 shows the functions $\cosh\left[\lambda\frac{x-\frac{1}{2}}{\mathrm{Kn}}\right], \sinh\left[\lambda\frac{x-\frac{1}{2}}{\mathrm{Kn}}\right]$ for a variety of Knudsen numbers, in order to emphasize the boundary layer structure of the solution (3.7). Indeed, these functions have the typical shape of a boundary layer, their largest values are found at the walls, and the curves decrease to zero within several mean free paths away from the walls. As Kn grows, the width of the boundary layers is growing as well. For Knudsen numbers above $\sim$0.05 one cannot speak of boundary layers anymore, since the functions $\cosh\left[\lambda\frac{x-\frac{1}{2}}{\mathrm{Kn}}\right], \sinh\left[\lambda\frac{x-\frac{1}{2}}{\mathrm{Kn}}\right]$ are non-zero anywhere in the region between the plates. In this case boundary effects have an important influence on the flow pattern. Note that we consider linear boundary layers, as solutions of linearized equations. These depend only on the Knudsen number, but, as a consequence of linearization, not on the Mach number.

For temperature, we find similar behavior: From the super-Burnett equations, we find

$$T_{|SB} = T_0 - \frac{4}{15}q_1\frac{x}{\mathrm{Kn}} + C\cos\left[\lambda_1\tfrac{x-\frac{1}{2}}{\mathrm{Kn}}\right] + D\sin\left[\lambda_1\tfrac{x-\frac{1}{2}}{\mathrm{Kn}}\right] + F\cosh\left[\lambda_2\tfrac{x-\frac{1}{2}}{\mathrm{Kn}}\right] + G\sinh\left[\lambda_2\tfrac{x-\frac{1}{2}}{\mathrm{Kn}}\right]$$

$$\text{with}\quad \lambda_1 = \sqrt{\tfrac{3\sqrt{53129}-201}{1216}} = 0.635,\ \lambda_2 = \sqrt{\tfrac{3\sqrt{53129}+201}{1216}} = 0.857\ ,$$

where the constants T_0, q_1, C, D, F, G must be obtained from boundary conditions. This solution correspond to the linear Fourier solution $T_0 - \frac{4}{15}q_1\frac{x}{\mathrm{Kn}}$ plus corrections, of which one is again periodic in space, while the other is of boundary layer type.

From the augmented Burnett equations, one finds

$$T = T_0 - \frac{4}{15}q_1\frac{x}{\mathrm{Kn}} + C\cosh\left[\gamma_1\tfrac{x-\frac{1}{2}}{\mathrm{Kn}}\right] + D\sinh\left[\gamma_1\tfrac{x-\frac{1}{2}}{\mathrm{Kn}}\right] + F\cosh\left[\gamma_2\tfrac{x-\frac{1}{2}}{\mathrm{Kn}}\right] + G\sinh\left[\gamma_2\tfrac{x-\frac{1}{2}}{\mathrm{Kn}}\right]$$

$$\text{with}\quad \gamma_1 = \sqrt{\tfrac{3\sqrt{5081}+303}{128}} = 2.009,\quad \gamma_2 = \sqrt{\tfrac{303-3\sqrt{5081}}{1216}} = 0.835\ ,$$

so that both corrections are of boundary layer type.

At this point of our arguments we can draw the following conclusions: (1) The super-Burnett equations lead to unphysical periodic solutions in steady state flows, and should not be considered for steady state problems. (2) The augmented Burnett equations seem to describe Knudsen boundary layers for velocity and temperature, and might be useful. The main point against them is that the terms of super-Burnett order that were used to augment the Burnett equations are not based on rational arguments: the coefficient $\frac{11}{16}$ instead of $-\frac{157}{16}$ in the equation for $q_{i|aB}$, (3.5)$_2$ stems from an erroneous computation in [15], and the coefficient $\frac{1}{6}$ instead of $-\frac{2}{3}$ in the equation for $\sigma_{12|aB}$, (3.5)$_1$, results from a wrong guess of the three dimensional structure of $\sigma_{ij}^{(a)}$ in (2.6), with a result that is not in agreement with the real super-Burnett equations (2.5). Polemically one could say that in the augmented Burnett equations the signs of those coefficients "that cause the trouble" are inverted, which results in good behavior of the equations, but is difficult if not impossible to justify by an argument based in physics. Another point against the augmented Burnett equations is that they, as we have said already above, are unstable with respect to local fluctuations at high frequencies [12].

4 Regularized 13 moment equations

The R13 equations were presented recently in [5,12], and [14]. Their original derivation in [5] is based on a regularization of Grad's 13 moment equations, where the regularizing terms result from a Chapman-Enskog expansion of moment equations for higher moments.

Only recently, Struchtrup was able to derive the R13 equations by a new argument, which is independent of Grad's method, but uses a careful analysis of the order of magnitude of the moments, and the influence of all terms in all moment equations on the conservation law [14].

Thus, the R13 equations have a rational background, in particular they contain no unknown coefficients and they are known in their full non-linear three dimensional form. They could be shown to include the Navier-Stokes, Burnett, and super-Burnett equations in their respective limit of the Knudsen number. However, as the discussion in [5,12] makes clear, they contain terms of arbitrary order in the Knudsen number, and these have a distinct influence on the solution behavior, in particular no instabilities occur. See the discussions in [5,12], and [14] for a thorough comparison of the methods of derivation for Grad equations, Burnett models, and the R13 equations.

The R13 method adds balance laws for stress and heat flux which read in linear, dimensionless form

$$\frac{\partial\sigma_{ij}}{\partial t}+\frac{4}{5}\frac{\partial q_{\langle i}}{\partial x_{j\rangle}}+2\frac{\partial v_{\langle i}}{\partial x_{j\rangle}}-2\mathrm{Kn}\frac{\partial}{\partial x_k}\frac{\partial\sigma_{\langle ij}}{\partial x_{k\rangle}}=-\frac{\sigma_{ij}}{\mathrm{Kn}}\ , \tag{4.1}$$
$$\frac{\partial q_i}{\partial t}+\frac{5}{2}\frac{\partial T}{\partial x_i}+\frac{\partial\sigma_{ik}}{\partial x_k}-\frac{12}{5}\mathrm{Kn}\frac{\partial}{\partial x_k}\frac{\partial q_{\langle i}}{\partial x_{k\rangle}}-2\mathrm{Kn}\frac{\partial}{\partial x_i}\frac{\partial q_k}{\partial x_k}=-\frac{2}{3}\frac{q_i}{\mathrm{Kn}}\ .$$

See [5,12] for the full non-linear system in three dimensions. A similar set of linear equations is presented by Karlin et al. [16], who, however, did not give explicit numerical expressions for the coefficients. For the steady Couette flow considered above, the linearized R13 equations (4.1,3.1) reduce to

$$\frac{\partial v}{\partial x}+\frac{2}{5}\frac{\partial q_2}{\partial x}=-\frac{\sigma_{12}}{\mathrm{Kn}}=const\ \ ,\ \ q_2=\frac{9}{5}\mathrm{Kn}^2\frac{\partial^2 q_2}{\partial x^2}\ ,$$
$$\frac{5}{2}\frac{\partial T}{\partial x}+\frac{\partial\sigma_{11}}{\partial x}=-\frac{2}{3}\frac{q_1}{\mathrm{Kn}}=const\ \ ,\ \ \sigma_{11}=\frac{6}{5}\mathrm{Kn}^2\frac{\partial^2\sigma_{11}}{\partial x^2}\ ,$$

so that velocity and temperature are obtained as

$$v(x)=v_0-\sigma_{12}\frac{x}{\mathrm{Kn}}-\frac{2}{5}q_2(x)\quad\text{with}\quad q_2(x)=A\sinh\left[\sqrt{\frac{5}{9}}\frac{x-\frac{1}{2}}{\mathrm{Kn}}\right]+B\cosh\left[\sqrt{\frac{5}{9}}\frac{x-\frac{1}{2}}{\mathrm{Kn}}\right],$$
$$T(x)=T_0-\frac{4}{15}q_1\frac{x}{\mathrm{Kn}}-\frac{2}{5}\sigma_{11}(x)\quad\text{with}\quad\sigma_{11}(x)=C\sinh\left[\sqrt{\frac{5}{6}}\frac{x-\frac{1}{2}}{\mathrm{Kn}}\right]+D\cosh\left[\sqrt{\frac{5}{6}}\frac{x-\frac{1}{2}}{\mathrm{Kn}}\right], \tag{4.2}$$

where v_0, σ_{12}, A, B and T_0, q_1, C, D are constants of integration. We can identify $-\frac{2}{5}q_2(x)$ and $-\frac{2}{5}\sigma_{11}(x)$ as the Knudsen boundary layers for velocity and temperature according to the R13 equations, and they are of the same form as those discussed above, and depicted in Fig. 1.

5 The heat flux parallel to the flow

A closer inspection of the last equations shows that the R13 equations predict the heat flux parallel to the flow as

$$q_{2|R13} = -\frac{9}{2}\mathrm{Kn}^2\frac{\partial^2 v}{\partial x^2} \ , \tag{5.1}$$

while the corresponding expression from the Burnett equations reads

$$q_{2|B} = \frac{3}{2}\mathrm{Kn}^2\frac{\partial^2 v}{\partial x^2} \ . \tag{5.2}$$

Note that the augmented Burnett equations and the super-Burnett equations agree with the Burnett equation up to the order of Kn^2, so that they also predict the result (5.2). Thus, we find different signs for q_2 between the R13 equations, and the Burnett equations.

In order to answer the question which sign relates heat flux and the second gradient of velocities in a rarefied gas, we use the results of a DSMC simulation for Couette flow, performed with the free code supplied by Bird [1]. For the interaction model in the DSMC simulation we considered the variable soft sphere model with the parameters for Maxwell molecules. We consider Couette flow at $\mathrm{Kn} = 0.1$ with dimensionless wall velocities $v(0) = 0$, $v(1) = 0.84$, and dimensionless wall temperatures $T(0) = T(1) = 1$. Bird's code requires physical data input (not dimensionless), and we used the following data: $T(0) = T(L) = T_0 = 273$K, $v(0) = 0$, $v(L) = 200$m/s, $\mu(T_0) = 1.955 \times 10^{-5}$Ns/m^2, $\rho_0 = 9.288 \times 10^{-6}$kg/m^3, $R = 0.208$kJ/kgK (Argon), and $L = 0.08833$m. Note that this data gives $\mathrm{Kn} = 0.1$ according to our definition in Eqn. (2.1), which differs from the definition given in [1].

The strong scatter in the DSMC results does not allow to compute the derivatives of the velocities, and therefore we base our argument on $(4.2)_1$. Solving for q_2 yields

$$q_{2|R13}(x) = -\frac{5}{2}\left[v(x) - v(0.5) + \sigma_{12}\frac{x-0.5}{\mathrm{Kn}}\right], \tag{5.3}$$

where we have used the point $x = 0.5$ to determine the constant v_0; note also that σ_{12} is a constant. We could write a similar equation for the super-Burnett equations by integrating $(3.4)_2$, but refrain from that since the super-Burnett equations, as we showed, yield periodic solutions, and are unphysical. Integrating the corresponding equation of the augmented Burnett equations $(3.5)_1$ yields with (5.2)

$$q_{2|aB} = 9\left[v(x) - v(0.5) + \sigma_{12|aB}\frac{x-0.5}{\mathrm{Kn}}\right] \ , \tag{5.4}$$

that is a similar curve, albeit with different sign and amplitude.

In Fig. 2, we show the heat flux q_2 as computed directly in the simulation, and as computed from (5.3), where we used the DSMC data for the evaluation of the right hand side. While $q_{2|R13}$ as given in (5.3) differs from the simulation value $q_{2|\mathrm{DSMC}}$, it is clear that the relation (5.3) yields the proper direction of q_2, while (5.4) would yield the opposite – wrong – direction. Note that our analysis is based on the linearized equations so that the difference between $q_{2|R13}$ and $q_{2|\mathrm{DSMC}}$ might be due to non-linear effects. The figure also shows the function $A\sinh\left[\sqrt{\frac{5}{9}}\frac{x-\frac{1}{2}}{\mathrm{Kn}}\right]$ with fitted amplitude A, and one can see that the heat flux $q_{2|\mathrm{DSMC}}$ indeed agrees well with the R13 prediction $(4.2)_1$.

6 Conclusions

We summarize our discussion of the Burnett, super-Burnett, and augmented Burnett equations by stating that neither of these theories should be considered for the description of transient or steady state processes in rarefied gases. All sets of equations exhibit instabilities in transient processes, while their predictions of steady state Couette flow lead to unphysical periodic solutions (super-Burnett), and the wrong sign of the heat flux parallel to the wall (all three).

The regularized 13 moment equations of Struchtrup and Torrilhon (R13), however, are superior on all counts: they are derived in a rational manner, are stable in time and space, and give predictions in agreement with (DSMC) experiments (see also [5,12]), including the proper behavior of the heat flux parallel to the flow.

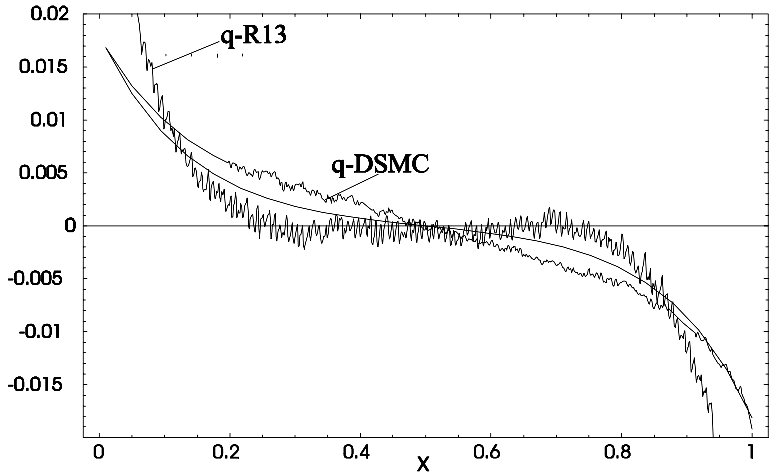

Fig. 2. $\mathrm{Kn} = 0.1$, q-DSMC: from DSMC simulation, q-R13: from DSMC result for velocity and (5.3). The thin line is the prediction of the R13 equations $q_2 = A \sinh\left[\sqrt{\frac{5}{9}}\frac{x-\frac{1}{2}}{\mathrm{Kn}}\right]$, see (4.2)

Moreover, when expanded in the Chapman-Enskog series, the R13 equations agree up to the super-Burnett order with the expansion of the Boltzmann equation. But we wish to emphasize that the good quality of the R13 equations is strongly influenced by the fact that they contain contributions of all powers in the Knudsen numbers, which, as becomes more and more obvious, are of great importance.

A full evaluation of the quality of the R13 equations will only be possible after a rational way to prescribe their boundary conditions is found (note that also for super-Burnett and augmented Burnett the boundary conditions are not known), and we hope to present these in the future.

Acknowledgements. This research was supported by the Natural Sciences and Engineering Research Council (NSERC). The author wishes to thank Adam Schuetze (University of Victoria) for providing the DSMC simulations, and Manuel Torrilhon (ETH Zurich) for stimulating discussions.

References

1. Bird, G.: Molecular gas dynamics and the direct simulation of gas flows. Clarendon Press, Oxford 1994
2. Chapman, S., Cowling, T.G.: *The Mathematical Theory of Non-Uniform Gases*, Cambridge University Press 1970
3. Shavaliyev,M.Sh.: Super-Burnett Corrections to the Stress Tensor and the Heat Flux in a Gas of Maxwellian Molecules. J. Appl. Maths. Mechs. **57**(3), 573–576 (1993)
4. Bobylev, A.V.: The Chapman-Enskog and Grad methods for solving the Boltzmann equation. Sov. Phys. Dokl. **27**, 29–31 (1982)
5. Struchtrup, H., Torrilhon, M.: Regularization of Grad's 13 Moment Equations: Derivation and Linear Analysis. Phys. Fluids **15**(9), 2668–2680 (2003)
6. Xue, H., Ji, H.M., Shu, C.: Analysis of micro-Couette flow using the Burnett equations. Int. J. Heat Mass Transfer **44**(21), 4139–4146 (2001)
7. Lockerby, D.A., Reese, J.M.: High resolution Burnett simulation of micro Couette flow and heat transfer. J. Comp. Phys. **188**, 333–347 (2003)
8. Xu, K.: Super-Burnett solutions for Poiseuille flow. Phys. Fluids **15**(7), 2077–2080 (2003)
9. Fiscko, K.A., Chapman, D.R.: Comparison of Burnett, Super-Burnett and Monte Carlo Solutions for Hypersonic Shock Structure. in *Proceedings of the 16th Symposium on Rarefied Gasdynamics* pp. 374-395, AIAA, Washington (1989)
10. Zhong, X., MacCormack, R.W., Chapman, D.R.: Stabilization of the Burnett Equations and Applications to High-Altitude Hypersonic Flows. AIAA 91-0770 (1991)
11. Zhong, X., MacCormack, R.W., Chapman, D.R.: Stabilization of the Burnett Equations and Applications to Hypersonic Flows. AIAA Journal **31**, 1036 (1993)
12. Torrilhon, M., Struchtrup, H.: Regularized 13-Moment-Equations: Shock Structure Calculations and Comparison to Burnett Models. J. Fluid Mech. **513**, 171–198 (2004)
13. Grad, H.: On the Kinetic Theory of Rarefied Gases. Comm. Pure Appl. Math. **2**, 325 (1949)
14. Struchtrup, H.: Stable transport equations for rarefied gases at high orders in the Knudsen number. Phys. Fluids **16**(11), 3921–3934 (2004)
15. Wang Chang, C.S.: On the theory of the thickness of weak shock waves. Studies in Statistical Mechanics V, 27–42, North Holland, Amsterdam (1970)
16. Karlin, I.V., Gorban, A.N., Dukek, G., Nonnenmacher, T.F.: Dynamic correction to moment approximations. Phys. Rev. E **57**(2), 1668–1672 (1998)